

# Features in the primordial spectrum and associated non-Gaussianities

L. Sriramkumar

Indian Institute of Technology Madras, Chennai

Astro-Cosmo @ Trivandrum, IISER, Thiruvananthapuram

November 18, 2011

# Proliferation of inflationary models<sup>1</sup>

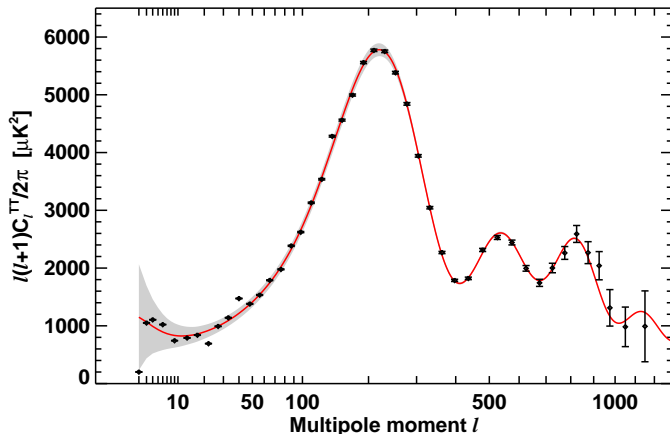
5-dimensional assisted inflation	extended open inflation	late-time mild inflation	pre-Big-Bang inflation
anisotropic brane inflation	extended warm inflation	low-scale inflation	primary inflation
anomaly-induced inflation	extra dimensional inflation	low-scale supergravity inflation	primordial inflation
assisted inflation	F-term inflation	M-theory inflation	quasi-open inflation
assisted chaotic inflation	F-term hybrid inflation	mass inflation	quintessential inflation
boundary inflation	false vacuum inflation	massive chaotic inflation	R-invariant topological inflation
brane inflation	false vacuum chaotic inflation	moduli inflation	rapid asymmetric inflation
brane-assisted inflation	fast-roll inflation	multi-scalar inflation	running inflation
brane gas inflation	first order inflation	multiple inflation	scalar-tensor gravity inflation
brane-antibrane inflation	gauged inflation	multiple-field slow-roll inflation	scalar-tensor stochastic inflation
braneworld inflation	generalised inflation	multiple-stage inflation	Seiberg-Witten inflation
Brans-Dicke chaotic inflation	generalized assisted inflation	natural inflation	single-bubble open inflation
Brans-Dicke inflation	generalized slow-roll inflation	natural Chaotic inflation	spinodal inflation
bulky brane inflation	gravity driven inflation	natural double inflation	stable starobinsky-type inflation
chaotic hybrid inflation	Hagedorn inflation	natural supergravity inflation	steady-state eternal inflation
chaotic inflation	higher-curvature inflation	new inflation	steep inflation
chaotic new inflation	hybrid inflation	next-to-minimal supersymmetric hybrid inflation	stochastic inflation
D-brane inflation	hyperextended inflation	non-commutative inflation	string-forming open inflation
D-term inflation	induced gravity inflation	non-slow-roll inflation	successful D-term inflation
dilaton-driven inflation	induced gravity open inflation	nonminimal chaotic inflation	supergravity inflation
dilaton-driven brane inflation	intermediate inflation	old inflation	supernatural inflation
double inflation	inverted hybrid inflation	open hybrid inflation	superstring inflation
double D-term inflation	isocurvature inflation	open inflation	supersymmetric hybrid inflation
dual inflation	K inflation	oscillating inflation	supersymmetric inflation
dynamical inflation	kinetic inflation	polynomial chaotic inflation	supersymmetric topological inflation
dynamical SUSY inflation	lambda inflation	polynomial hybrid inflation	supersymmetric new inflation
eternal inflation	large field inflation	power-law inflation	synergistic warm inflation
extended inflation	late D-term inflation		TeV-scale hybrid inflation

A (partial?) list of ever-increasing number of inflationary models. May be, we should look for models that permit deviations from the standard picture of slow roll inflation.

<sup>1</sup>From E. P. S. Shellard, *The future of cosmology: Observational and computational prospects*, in *The Future of Theoretical Physics and Cosmology*, Eds. G. W. Gibbons, E. P. S. Shellard and S. J. Rankin (Cambridge University Press, Cambridge, England, 2003).



# Angular power spectrum from the WMAP 7-year data<sup>2</sup>

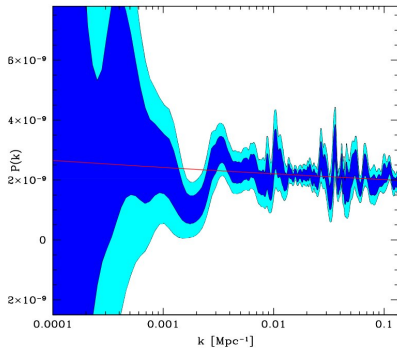
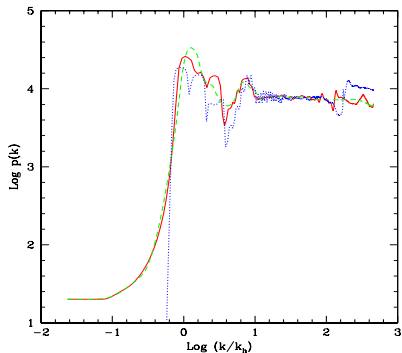


The WMAP 7-year data for the CMB TT angular power spectrum (the black dots with error bars) and the theoretical, best fit  $\Lambda$ CDM model with a power law primordial spectrum (the solid red curve). Note the outliers near the multipoles  $\ell = 2, 22$  and  $40$ .

<sup>2</sup>D. Larson *et al.*, *Astrophys. J. Suppl.* **192**, 16 (2011).



# Reconstructing the primordial spectrum



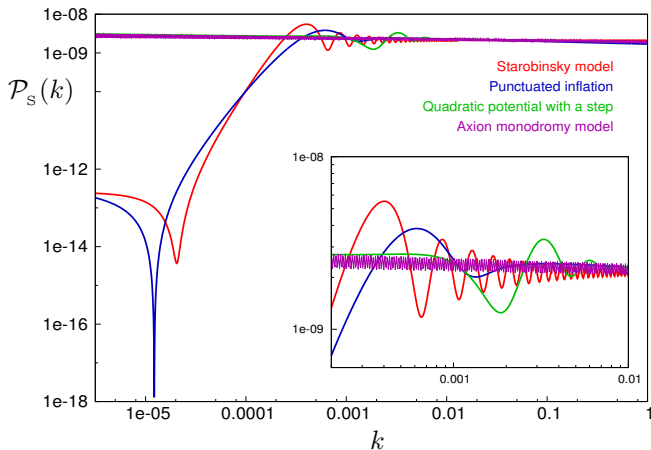
Reconstructed primordial spectra, obtained upon assuming the concordant background  $\Lambda$ CDM model. The recovered spectrum on the left improves the fit to the WMAP 3-year data by  $\Delta\chi_{\text{eff}}^2 \simeq 15$ , with respect to the best fit power law spectrum<sup>3</sup>. The spectrum on the right has been recovered from a variety of CMB datasets, including the WMAP 5-year data<sup>4</sup>.

<sup>3</sup>A. Shafieloo, T. Souradeep, P. Manimaran, P. K. Panigrahi and R. Rangarajan, *Phys. Rev. D* **75**, 123502 (2007).

<sup>4</sup>G. Nicholson and C. R. Contaldi, *JCAP* **0907**, 011 (2009).



# Inflationary models leading to features<sup>5</sup>



The scalar power spectra in a few different inflationary models that lead to a better fit to the CMB data than the conventional power law spectrum.

<sup>5</sup>R. K. Jain, P. Chingangbam, J.-O. Gong, L. Sriramkumar and T. Souradeep, JCAP **0901**, 009 (2009);  
 D. K. Hazra, M. Aich, R. K. Jain, L. Sriramkumar and T. Souradeep, JCAP **1010**, 008 (2010);  
 M. Aich, D. K. Hazra, L. Sriramkumar and T. Souradeep, arXiv:1106.2798v1 [astro-ph.CO].



# 'Large' non-Gaussianities and its possible implications

- The WMAP 7-year data constrains the non-Gaussianity parameter  $f_{\text{NL}}$  to be  $f_{\text{NL}} = 32 \pm 21$  in the local limit, at 68% confidence level<sup>6</sup>.
- If forthcoming missions such as Planck detect a large level of non-Gaussianity, as suggested by the above mean value of  $f_{\text{NL}}$ , then it can result in a substantial tightening in the constraints on the various inflationary models. For example, canonical scalar field models that lead to a nearly scale invariant primordial spectrum contain only a small amount of non-Gaussianity and, hence, will cease to be viable<sup>7</sup>.
- However, it is known that primordial spectra with features can lead to reasonably large non-Gaussianities<sup>8</sup>. Therefore, if the non-Gaussianity parameter  $f_{\text{NL}}$  indeed proves to be large, then either one has to reconcile with the fact that the primordial spectrum contains features or we have to turn our attention to non-canonical scalar field models such as, say, D brane inflation models<sup>9</sup>.

<sup>6</sup>E. Komatsu *et al.*, *Astrophys. J. Suppl.* **192**, 18 (2011).

<sup>7</sup>J. Maldacena, *JHEP* **05**, 013 (2003).

<sup>8</sup>See, for instance, X. Chen, R. Easther and E. A. Lim, *JCAP* **0706**, 023 (2007).

<sup>9</sup>See, for example, X. Chen, M.-x. Huang, S. Kachru and G. Shiu, *JCAP* **0701**, 002 (2007).



# This talk is based on

- J. Martin and L. Sriramkumar, *The scalar bi-spectrum in the Starobinsky model: The equilateral case*, arXiv:1109.5838v1 [astro-ph.CO].
- D. K. Hazra, L. Sriramkumar and J. Martin, *On the discriminating power of  $f_{\text{NL}}$* , In preparation.



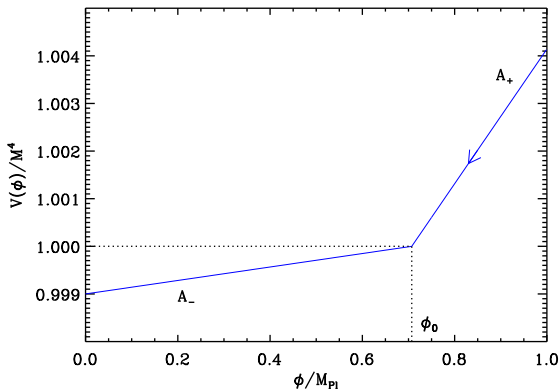
# Outline of the talk

- 1 The scalar power spectrum in the Starobinsky model
- 2 The definition of the non-Gaussianity parameter  $f_{\text{NL}}$
- 3 The method for evaluating  $f_{\text{NL}}$
- 4  $f_{\text{NL}}$  in the Starobinsky model (in the equilateral limit)
- 5 Can  $f_{\text{NL}}$  help in discriminating between inflationary models?
- 6 Summary





# The Starobinsky model<sup>10</sup>



The Starobinsky model involves the canonical scalar field which is described by the potential

$$V(\phi) = \begin{cases} V_0 + A_+ (\phi - \phi_0) & \text{for } \phi > \phi_0, \\ V_0 + A_- (\phi - \phi_0) & \text{for } \phi < \phi_0. \end{cases}$$

<sup>10</sup>A. A. Starobinsky, Sov. Phys. JETP Lett. **55**, 489 (1992).



# Assumptions and properties

- It is assumed that the constant  $V_0$  is the dominant term in the potential for a range of  $\phi$  near  $\phi_0$ . As a result, over the domain of our interest, the expansion is of the de Sitter form corresponding to a Hubble parameter  $H_0$  determined by  $V_0$ .
- The scalar field rolls slowly until it reaches the discontinuity in the potential. It then fast rolls for a brief period as it crosses the discontinuity before slow roll is restored again.
- Since  $V_0$  is dominant, the first slow roll parameter  $\epsilon_1$  remains small even during the transition. This property allows the background to be evaluated analytically to a good approximation.



# Analytic expressions for the slow roll parameters

Under the assumptions and approximations described above, the slow roll parameters remain small before the transition.



# Analytic expressions for the slow roll parameters

Under the assumptions and approximations described above, the slow roll parameters remain small before the transition.

One can show that, after the transition, the evolution of the first slow roll parameter  $\epsilon_1$  can be expressed in terms of the number of e-folds  $N$  as follows:

$$\epsilon_{1-} \simeq \frac{A_-^2}{18 M_{\text{Pl}}^2 H_0^4} \left[ 1 - \frac{\Delta A}{A_-} e^{-3(N-N_0)} \right]^2,$$

where  $\Delta A = (A_- - A_+)$ , while  $N_0$  is the e-fold at which the field crosses the discontinuity.



# Analytic expressions for the slow roll parameters

Under the assumptions and approximations described above, the slow roll parameters remain small before the transition.

One can show that, after the transition, the evolution of the first slow roll parameter  $\epsilon_{1-}$  can be expressed in terms of the number of e-folds  $N$  as follows:

$$\epsilon_{1-} \simeq \frac{A_-^2}{18 M_{\text{Pl}}^2 H_0^4} \left[ 1 - \frac{\Delta A}{A_-} e^{-3(N-N_0)} \right]^2,$$

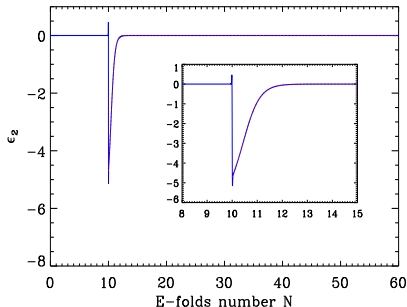
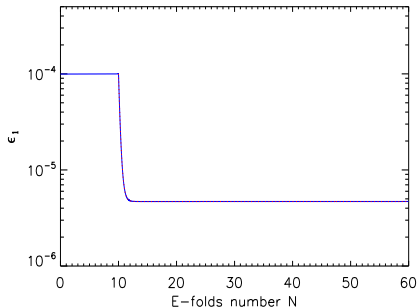
where  $\Delta A = (A_- - A_+)$ , while  $N_0$  is the e-fold at which the field crosses the discontinuity.

It is found that, *immediately after the transition*, the second slow roll parameter  $\epsilon_{2-}$  is given by

$$\epsilon_{2-} \simeq \frac{6 \Delta A}{A_-} \frac{e^{-3(N-N_0)}}{1 - (\Delta A/A_-) e^{-3(N-N_0)}}.$$



# Evolution of the slow roll parameters



The evolution of the first slow roll parameter  $\epsilon_1$  on the left, and the second slow roll parameter  $\epsilon_2$  on the right in the Starobinsky model. While the blue curves describe the numerical results, the dotted red curves represent the analytical expressions mentioned in the previous slide.



# The modes before and after the transition

It can be shown that, under the assumptions that one is working with, the quantity  $z = a M_{\text{Pl}} \sqrt{2\epsilon_1}$ , which determines the evolution of the modes, say,  $f_k$ , associated with the curvature perturbation  $\mathcal{R}_k$ , simplifies to

$$z''/z \simeq 2\mathcal{H}^2$$

both before *as well as* after the transition with the overprime denoting the derivative with respect to the conformal time, while  $\mathcal{H}$  is the conformal Hubble parameter.



# The modes before and after the transition

It can be shown that, under the assumptions that one is working with, the quantity  $z = a M_{\text{Pl}} \sqrt{2\epsilon_1}$ , which determines the evolution of the modes, say,  $f_k$ , associated with the curvature perturbation  $\mathcal{R}_k$ , simplifies to

$$z''/z \simeq 2\mathcal{H}^2$$

both before *as well as* after the transition with the overprime denoting the derivative with respect to the conformal time, while  $\mathcal{H}$  is the conformal Hubble parameter.

As a result, while the solution to the Mukhanov-Sasaki variable  $v_k = (z f_k)$  corresponding to the Bunch-Davies vacuum before the transition is given by

$$v_k^+(\eta) = \frac{1}{\sqrt{2k}} \left(1 - \frac{i}{k\eta}\right) e^{-ik\eta},$$

after the transition, it can be expressed as a linear combination of the positive and the negative frequency modes as follows:

$$v_k^-(\eta) = \frac{\alpha_k}{\sqrt{2k}} \left(1 - \frac{i}{k\eta}\right) e^{-ik\eta} + \frac{\beta_k}{\sqrt{2k}} \left(1 + \frac{i}{k\eta}\right) e^{ik\eta},$$

where  $\alpha_k$  and  $\beta_k$  are the usual Bogoliubov coefficients.





# The scalar power spectrum in the Starobinsky model

The Bogoliubov coefficients  $\alpha_k$  and  $\beta_k$  can be obtained by matching the mode  $v_k$  and its derivative at the transition.



# The scalar power spectrum in the Starobinsky model

The Bogoliubov coefficients  $\alpha_k$  and  $\beta_k$  can be obtained by matching the mode  $v_k$  and its derivative at the transition.

The scalar power spectrum, given by

$$\mathcal{P}_s(k) = (k^3/2\pi^2) |f_k|^2 = (k^3/2\pi^2) (|v_k|/z)^2,$$

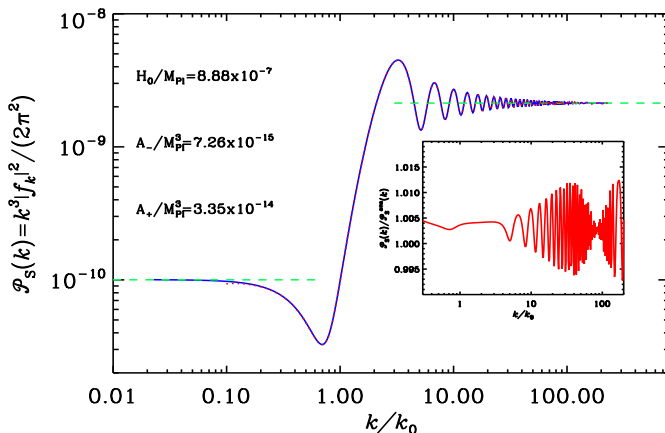
can be evaluated at late times to be

$$\begin{aligned} \mathcal{P}_s(k) = \left( \frac{9 H_0^6}{4 \pi^2 A_-^2} \right) \left\{ 1 - \frac{3 \Delta A k_0}{A_+ k} \left[ \left( 1 - \frac{k_0^2}{k^2} \right) \sin \left( \frac{2k}{k_0} \right) + \frac{2k_0}{k} \cos \left( \frac{2k}{k_0} \right) \right] \right. \\ \left. + \frac{9 \Delta A^2 k_0^2}{2 A_+^2 k^2} \left( 1 + \frac{k_0^2}{k^2} \right) \left[ \left( 1 + \frac{k_0^2}{k^2} \right) - \frac{2k_0}{k} \sin \left( \frac{2k}{k_0} \right) \right. \right. \\ \left. \left. + \left( 1 - \frac{k_0^2}{k^2} \right) \cos \left( \frac{2k}{k_0} \right) \right] \right\}, \end{aligned}$$

where the quantity  $k_0$  is the wavenumber of the mode that leaves the Hubble radius when the field crosses the discontinuity. Note that the power spectrum depends on the wavenumber only through the ratio  $(k/k_0)$ .



# Comparison with the numerical result



The scalar power spectrum in the Starobinsky model. While the blue solid curve denotes the analytic result, the red dots represent the corresponding numerical scalar power spectrum that has been obtained through an exact integration of the background as well as the perturbations.



# The scalar bi-spectrum

The scalar bi-spectrum  $\mathcal{B}_S(\mathbf{k}_1, \mathbf{k}_2, \mathbf{k}_3)$  is related to the three point correlation function of the Fourier modes of the curvature perturbation, evaluated towards the end of inflation, say, at the conformal time  $\eta_e$ , as follows<sup>11</sup>:

$$\langle \hat{\mathcal{R}}_{\mathbf{k}_1}(\eta_e) \hat{\mathcal{R}}_{\mathbf{k}_2}(\eta_e) \hat{\mathcal{R}}_{\mathbf{k}_3}(\eta_e) \rangle = (2\pi)^3 \mathcal{B}_S(\mathbf{k}_1, \mathbf{k}_2, \mathbf{k}_3) \delta^{(3)}(\mathbf{k}_1 + \mathbf{k}_2 + \mathbf{k}_3).$$

For convenience, we shall set

$$\mathcal{B}_S(\mathbf{k}_1, \mathbf{k}_2, \mathbf{k}_3) = (2\pi)^{-9/2} G(\mathbf{k}_1, \mathbf{k}_2, \mathbf{k}_3).$$

<sup>11</sup>D. Larson *et al.*, *Astrophys. J. Suppl.* **192**, 16 (2011);  
E. Komatsu *et al.*, *Astrophys. J. Suppl.* **192**, 18 (2011).



# The introduction of $f_{\text{NL}}$

The observationally relevant non-Gaussianity parameter  $f_{\text{NL}}$  is introduced through the equation<sup>12</sup>

$$\mathcal{R}(\eta, \mathbf{x}) = \mathcal{R}^{\text{G}}(\eta, \mathbf{x}) - \frac{3f_{\text{NL}}}{5} [\mathcal{R}^{\text{G}}(\eta, \mathbf{x})]^2,$$

where  $\mathcal{R}^{\text{G}}$  denotes the Gaussian quantity, and the factor of  $(3/5)$  arises due to the relation between the Bardeen potential and the curvature perturbation during the matter dominated epoch.

---

<sup>12</sup>J. Maldacena, JHEP **0305**, 013 (2003);  
S. Hannestad, T. Haugbolle, P. R. Jarnhus and M. S. Sloth, JCAP **1006**, 001 (2010).



# The introduction of $f_{\text{NL}}$

The observationally relevant non-Gaussianity parameter  $f_{\text{NL}}$  is introduced through the equation<sup>12</sup>

$$\mathcal{R}(\eta, \mathbf{x}) = \mathcal{R}^{\text{G}}(\eta, \mathbf{x}) - \frac{3 f_{\text{NL}}}{5} [\mathcal{R}^{\text{G}}(\eta, \mathbf{x})]^2,$$

where  $\mathcal{R}^{\text{G}}$  denotes the Gaussian quantity, and the factor of  $(3/5)$  arises due to the relation between the Bardeen potential and the curvature perturbation during the matter dominated epoch.

It ought to be emphasized here that the non-Gaussianity parameter  $f_{\text{NL}}$  has been introduced through the above equation with the local limit in mind.

In Fourier space, the above equation can be written as

$$\mathcal{R}_{\mathbf{k}} = \mathcal{R}_{\mathbf{k}}^{\text{G}} - \frac{3 f_{\text{NL}}}{5} \int \frac{d^3 \mathbf{p}}{(2\pi)^{3/2}} \mathcal{R}_{\mathbf{p}}^{\text{G}} \mathcal{R}_{\mathbf{k}-\mathbf{p}}^{\text{G}}.$$

<sup>12</sup>J. Maldacena, JHEP **0305**, 013 (2003);

S. Hannestad, T. Haugbolle, P. R. Jarnhus and M. S. Sloth, JCAP **1006**, 001 (2010).



# The introduction of $f_{\text{NL}}$ . . . continued

Using the above relation and Wick's theorem, one can arrive at the three point correlation of the curvature perturbation in Fourier space in terms of the parameter  $f_{\text{NL}}$ . It is found to be

$$\langle \mathcal{R}_{\mathbf{k}_1} \mathcal{R}_{\mathbf{k}_2} \mathcal{R}_{\mathbf{k}_3} \rangle = - \left( \frac{3 f_{\text{NL}}}{10} \right) (2\pi)^4 (2\pi)^{-3/2} \left( \frac{1}{k_1^3 k_2^3 k_3^3} \right) \delta^{(3)}(\mathbf{k}_1 + \mathbf{k}_2 + \mathbf{k}_3) \\ \times [k_1^3 \mathcal{P}_s(k_2) \mathcal{P}_s(k_3) + \text{two permutations}] .$$



# The relation between $f_{\text{NL}}$ and the bi-spectrum

Upon using the above expression for the three point function of the curvature perturbation and the definition of the bi-spectrum, we can, in turn, arrive at the following relation:

$$\begin{aligned}
 f_{\text{NL}} &= - \left( \frac{10}{3} \right) (2\pi)^{-4} (2\pi)^{9/2} (k_1^3 k_2^3 k_3^3) \mathcal{B}_S(\mathbf{k}_1, \mathbf{k}_2, \mathbf{k}_3) \\
 &\quad \times [k_1^3 \mathcal{P}_S(k_2) \mathcal{P}_S(k_3) + \text{two permutations}]^{-1} \\
 &= - \left( \frac{10}{3} \right) (2\pi)^{-4} (k_1^3 k_2^3 k_3^3) G(\mathbf{k}_1, \mathbf{k}_2, \mathbf{k}_3) \\
 &\quad \times [k_1^3 \mathcal{P}_S(k_2) \mathcal{P}_S(k_3) + \text{two permutations}]^{-1}.
 \end{aligned}$$





# The relation between $f_{\text{NL}}$ and the bi-spectrum

Upon using the above expression for the three point function of the curvature perturbation and the definition of the bi-spectrum, we can, in turn, arrive at the following relation:

$$\begin{aligned}
 f_{\text{NL}} &= - \left( \frac{10}{3} \right) (2\pi)^{-4} (2\pi)^{9/2} (k_1^3 k_2^3 k_3^3) \mathcal{B}_S(\mathbf{k}_1, \mathbf{k}_2, \mathbf{k}_3) \\
 &\quad \times [k_1^3 \mathcal{P}_S(k_2) \mathcal{P}_S(k_3) + \text{two permutations}]^{-1} \\
 &= - \left( \frac{10}{3} \right) (2\pi)^{-4} (k_1^3 k_2^3 k_3^3) G(\mathbf{k}_1, \mathbf{k}_2, \mathbf{k}_3) \\
 &\quad \times [k_1^3 \mathcal{P}_S(k_2) \mathcal{P}_S(k_3) + \text{two permutations}]^{-1}.
 \end{aligned}$$

In the equilateral limit (i.e. when  $\mathbf{k}_1 = \mathbf{k}_2 = \mathbf{k}_3$ ), this expression for  $f_{\text{NL}}$  simplifies to

$$f_{\text{NL}}^{\text{eq}} = - \left( \frac{10}{9} \right) (2\pi)^{-4} \left( \frac{k^6 G(k)}{\mathcal{P}_S^2(k)} \right).$$



# The action at the cubic order<sup>13</sup>

It can be shown that the third order term in the action describing the curvature perturbations is given by

$$\mathcal{S}_3[\mathcal{R}] = M_{\text{Pl}}^2 \int d\eta \int d^3\mathbf{x} \left[ a^2 \epsilon_1^2 \mathcal{R} \mathcal{R}'^2 + a^2 \epsilon_1^2 \mathcal{R} (\partial\mathcal{R})^2 - 2 a \epsilon_1 \mathcal{R}' (\partial^i \mathcal{R}) (\partial_i \chi) \right. \\ \left. + \frac{a^2}{2} \epsilon_1 \epsilon_2' \mathcal{R}^2 \mathcal{R}' + \frac{\epsilon_1}{2} (\partial^i \mathcal{R}) (\partial_i \chi) (\partial^2 \chi) + \frac{\epsilon_1}{4} (\partial^2 \mathcal{R}) (\partial\chi)^2 + \mathcal{F} \left( \frac{\delta\mathcal{L}_2}{\delta\mathcal{R}} \right) \right],$$

where  $\mathcal{F}(\delta\mathcal{L}_2/\delta\mathcal{R})$  denotes terms involving the variation of the second order action with respect to  $\mathcal{R}$ , while  $\chi$  is related to the curvature perturbation  $\mathcal{R}$  through the relations

$$\Lambda = a \epsilon_1 \mathcal{R}' \quad \text{and} \quad \partial^2 \chi = \Lambda.$$

<sup>13</sup> J. Maldacena, JHEP **0305**, 013 (2003);  
 D. Seery and J. E. Lidsey, JCAP **0506**, 003 (2005);  
 X. Chen, M.-x. Huang, S. Kachru and G. Shiu, JCAP **0701**, 002 (2007).



# Evaluating the bi-spectrum

At the leading order in the perturbations, one then finds that the three point correlation in Fourier space is described by the integral

$$\begin{aligned} & \langle \hat{\mathcal{R}}_{\mathbf{k}_1}(\eta_e) \hat{\mathcal{R}}_{\mathbf{k}_2}(\eta_e) \hat{\mathcal{R}}_{\mathbf{k}_3}(\eta_e) \rangle \\ &= -i \int_{\eta_i}^{\eta_e} d\eta a(\eta) \left\langle \left[ \hat{\mathcal{R}}_{\mathbf{k}_1}(\eta_e) \hat{\mathcal{R}}_{\mathbf{k}_2}(\eta_e) \hat{\mathcal{R}}_{\mathbf{k}_3}(\eta_e), \hat{H}_I(\eta) \right] \right\rangle, \end{aligned}$$

where  $\hat{H}_I$  is the operator corresponding to the above third order action, while  $\eta_i$  is the time at which the initial conditions are imposed on the modes when they are well inside the Hubble radius, and  $\eta_e$  denotes a very late time, say, close to when inflation ends.

Note that, while the square brackets imply the commutation of the operators, the angular brackets denote the fact that the correlations are evaluated in the initial vacuum state (viz. the Bunch-Davies vacuum in the situation of our interest).



# Evaluating the bi-spectrum . . . continued

In the equilateral limit, the quantity  $G(k)$ , evaluated towards the end of inflation at the conformal time  $\eta = \eta_e$ , can be written as

$$G(k) \equiv \sum_{C=1}^7 G_C(k) = M_{\text{Pl}}^2 \sum_{C=1}^6 [f_k^3(\eta_e) \mathcal{G}_C(k) + f_k^{*3}(\eta_e) \mathcal{G}_C^*(k)] + G_7(k),$$

where the quantities  $\mathcal{G}_C(k)$  are integrals that correspond to six terms that arise in the action at the third order in the perturbations, while, recall that,  $f_k$  are the modes associated with the curvature perturbation  $\mathcal{R}_k$ .

The additional, seventh term  $G_7$  arises due to a field redefinition, and its contribution is given by<sup>14</sup>

$$G_7(k) = \frac{3 \epsilon_2(\eta_e)}{2} |f_k(\eta_e)|^4.$$

<sup>14</sup> J. Maldacena, JHEP **0305**, 013 (2003);  
 D. Seery and J. E. Lidsey, JCAP **0506**, 003 (2005);  
 X. Chen, M.-x. Huang, S. Kachru and G. Shiu, JCAP **0701**, 002 (2007).



# Evaluating $f_{\text{NL}}$ in the Starobinsky model

When there exist deviations from slow roll, it is often found that the fourth term  $\mathcal{G}_4$  provides the dominant contribution to  $f_{\text{NL}}$ .

It is described by the following integral

$$\mathcal{G}_4(k) = 3i \int_{\eta_i}^{\eta_e} d\eta a^2 \epsilon_1 \epsilon_2' f_k^{*2} f_k'^*$$

In the case of the Starobinsky model, as  $\epsilon_2$  is a constant before the transition,  $\epsilon_2'$  vanishes, and hence the above integral  $\mathcal{G}_4$  is non-zero only post-transition.



# Evaluating $f_{\text{NL}}$ in the Starobinsky model

When there exist deviations from slow roll, it is often found that the fourth term  $\mathcal{G}_4$  provides the dominant contribution to  $f_{\text{NL}}$ .

It is described by the following integral

$$\mathcal{G}_4(k) = 3i \int_{\eta_i}^{\eta_e} d\eta a^2 \epsilon_1 \epsilon_2' f_k^{*2} f_k'^*$$

In the case of the Starobinsky model, as  $\epsilon_2$  is a constant before the transition,  $\epsilon_2'$  vanishes, and hence the above integral  $\mathcal{G}_4$  is non-zero only post-transition.

We find that the integral involved can be computed analytically.



# Evaluating $f_{\text{NL}}$ in the Starobinsky model

When there exist deviations from slow roll, it is often found that the fourth term  $\mathcal{G}_4$  provides the dominant contribution to  $f_{\text{NL}}$ .

It is described by the following integral

$$\mathcal{G}_4(k) = 3i \int_{\eta_i}^{\eta_e} d\eta a^2 \epsilon_1 \epsilon_2' f_k^{*2} f_k'^*.$$

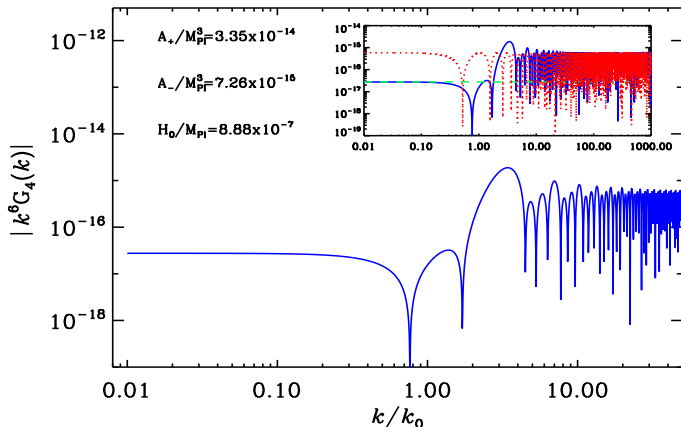
In the case of the Starobinsky model, as  $\epsilon_2$  is a constant before the transition,  $\epsilon_2'$  vanishes, and hence the above integral  $\mathcal{G}_4$  is non-zero only post-transition.

We find that the integral involved can be computed analytically.

In fact, with some effort, analytic expressions can be arrived at for all the  $\mathcal{G}_n$ .



# The dominant contribution in the Starobinsky model

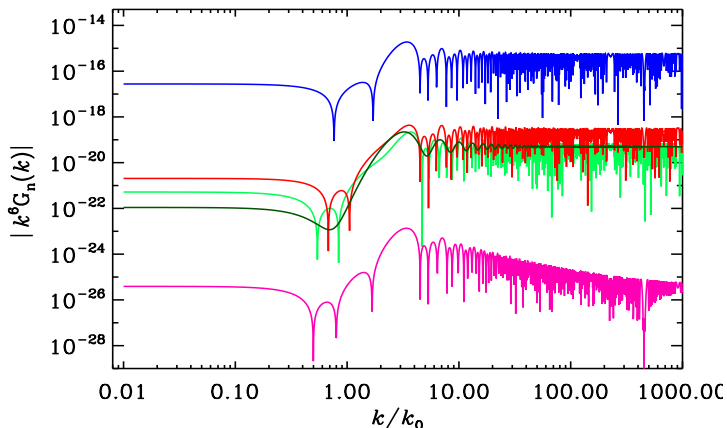


The absolute value of the quantity  $[k^6 G_4]$  has been plotted as a function of  $(k/k_0)$  (the blue curve). We have worked with the same values of  $A_+$ ,  $A_-$  and  $V_0$  as in the earlier figure wherein we had plotted the power spectrum. The green and the red curves in the inset represent the limiting values for  $k \ll k_0$  and  $k \gg k_0$ , respectively.



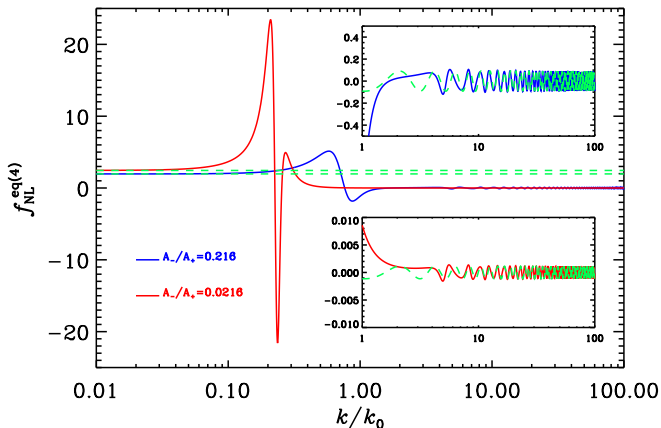


# The different contributions



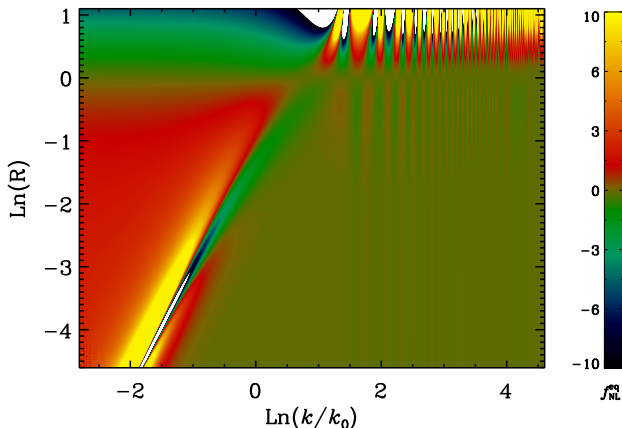
The quantities  $k^6$  times the absolute values of  $G_1 + G_3$  (in light green),  $G_2$  (in red),  $G_4$  (in blue),  $G_5 + G_6$  (in purple) and  $G_7$  (in dark green) have been plotted as a function of  $(k/k_0)$  for the Starobinsky model. We have worked with the same values of the parameters as in the previous three figures.



$f_{NL}^{eq}$  due to the dominant contribution

The non-Gaussianity parameter  $f_{NL}^{eq}$  due to the dominant term in the Starobinsky model, plotted as a function of  $(k/k_0)$  for  $(A_-/A_+) = 0.216$  and  $(A_-/A_+) = 0.0216$ . Larger the difference between  $A_-$  and  $A_+$ , larger is the corresponding  $f_{NL}^{eq}$ .

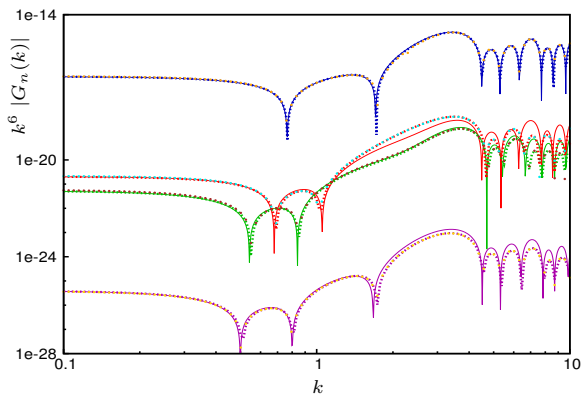


$f_{NL}^{eq}$  for a range of values of the parameters

The non-Gaussianity parameter  $f_{NL}^{eq}$  due to the dominant contribution in the Starobinsky model, plotted as a function of  $(k/k_0)$  and the ratio  $R = (A_-/A_+)$ . The white contours indicate regions wherein  $f_{NL}^{eq}$  can be as large as 50. Note that, provided  $R$  is reasonably small,  $f_{NL}^{eq}$  can be of the order of 20 or so, as is indicated by the currently observed mean value.

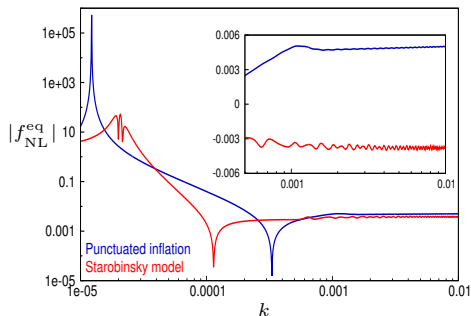
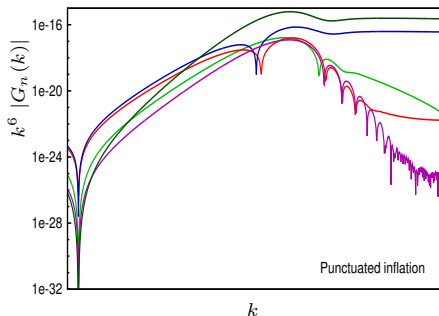


# Calibrating using the Starobinsky model



A comparison of the analytical expressions in the Starobinsky model with the corresponding numerical results. The solid curves represent the analytical expressions that we discussed earlier, while the dashed curves denote the numerical results computed using a Fortran 90 code. The dots of an alternate color denote the corresponding numerical values that have been arrived at independently using a Mathematica code.



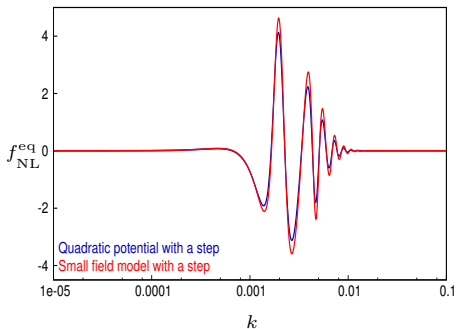
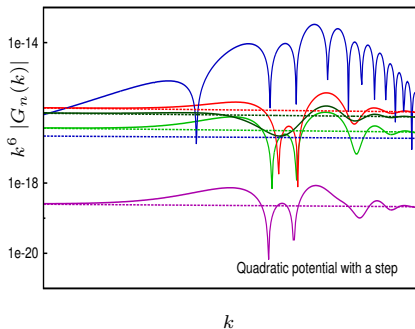
$f_{NL}^{eq}$  in punctuated inflation<sup>15</sup>

The contributions due to the various terms (on the left), and the absolute value of  $f_{NL}^{eq}$  due to the dominant contribution (on the right), in the punctuated inflationary scenario. The absolute value of  $f_{NL}^{eq}$  in a Starobinsky model that closely resembles the power spectrum in punctuated inflation has also been displayed. Note that  $f_{NL}^{eq}$  can become rather large in punctuated inflation. The large difference in  $f_{NL}^{eq}$  between punctuated inflation and the Starobinsky model can be attributed to the considerable difference in the background dynamics.

<sup>15</sup>R. K. Jain, P. Chingangbam, J.-O. Gong, L. Sriramkumar and T. Souradeep, JCAP **0901**, 009 (2009);  
R. K. Jain, P. Chingangbam, L. Sriramkumar and T. Souradeep, Phys. Rev. D **82**, 023509 (2010).



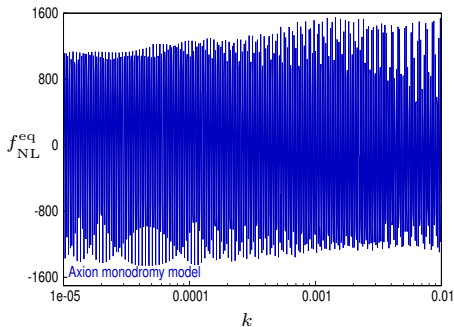
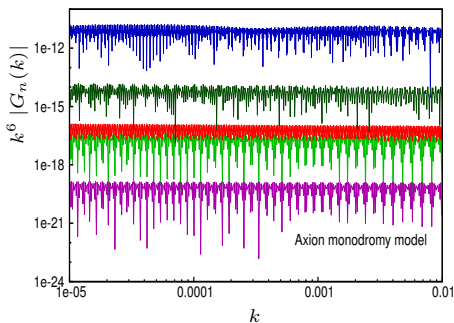
# Models with a step in the inflaton potential<sup>16</sup>



The contributions due to the various terms (on the left) and  $f_{NL}^{eq}$  due to the dominant contribution (on the right) when a step has been introduced in the popular chaotic inflationary model involving the quadratic potential. The  $f_{NL}^{eq}$  that arises in a small field model with a step has also been illustrated. The background dynamics in these two models are very similar, which lead to almost the same  $f_{NL}^{eq}$ .

<sup>16</sup>D. K. Hazra, M. Aich, R. K. Jain, L. Sriramkumar and T. Souradeep, JCAP **1010**, 008 (2010).



Oscillating inflation potentials<sup>17</sup>

The contributions due to the various terms (on the left) and  $f_{NL}^{eq}$  due to the dominant contribution (on the right) in the axion monodromy model. The model is described by a linear potential with superposed modulations. These modulations give rise to a certain resonant behavior, leading to a large  $f_{NL}^{eq}$ .

In contrast, oscillations introduced in the quadratic potential in a certain fashion do not result in such a large level of non-Gaussianity.

<sup>17</sup>R. Flauger, L. McAllister, E. Pajer, A. Westphal and G. Xu, JCAP **1006**, 009 (2010);  
M. Aich, D. K. Hazra, L. Sriramkumar and T. Souradeep, arXiv:1106.2798v1 [astro-ph.CO].



# Summary

- Remarkably, we find that, for a certain range of values of the parameters involved, the non-Gaussianity parameter  $f_{NL}^{eq}$  can be evaluated analytically, to a good accuracy (as is confirmed by comparison with numerical computations) in the Starobinsky model.





# Summary

- Remarkably, we find that, for a certain range of values of the parameters involved, the non-Gaussianity parameter  $f_{\text{NL}}^{\text{eq}}$  can be evaluated analytically, to a good accuracy (as is confirmed by comparison with numerical computations) in the Starobinsky model.
- Interestingly, for suitably small values of  $R = (A_-/A_+)$ ,  $f_{\text{NL}}^{\text{eq}}$  in the Starobinsky model can be as large as indicated by the currently observed mean values.



# Summary

- Remarkably, we find that, for a certain range of values of the parameters involved, the non-Gaussianity parameter  $f_{\text{NL}}^{\text{eq}}$  can be evaluated analytically, to a good accuracy (as is confirmed by comparison with numerical computations) in the Starobinsky model.
- Interestingly, for suitably small values of  $R = (A_-/A_+)$ ,  $f_{\text{NL}}^{\text{eq}}$  in the Starobinsky model can be as large as indicated by the currently observed mean values.
- The analytic results obtained in the case of the Starobinsky model can be utilized to calibrate numerical codes, thereby permitting the computation of bi-spectrum in a wide variety of inflationary models that contain departures from slow roll.



# Summary

- Remarkably, we find that, for a certain range of values of the parameters involved, the non-Gaussianity parameter  $f_{\text{NL}}^{\text{eq}}$  can be evaluated analytically, to a good accuracy (as is confirmed by comparison with numerical computations) in the Starobinsky model.
- Interestingly, for suitably small values of  $R = (A_-/A_+)$ ,  $f_{\text{NL}}^{\text{eq}}$  in the Starobinsky model can be as large as indicated by the currently observed mean values.
- The analytic results obtained in the case of the Starobinsky model can be utilized to calibrate numerical codes, thereby permitting the computation of bi-spectrum in a wide variety of inflationary models that contain departures from slow roll.
- We find that certain differences in the background dynamics—reflected in the behavior of the slow roll parameters—can lead to a reasonably large difference in the  $f_{\text{NL}}^{\text{eq}}$  generated by the competing models.



Thank you for your attention